Organic & Biomolecular Chemistry

ROYAL SOCIETY OF CHEMISTRY

PAPER

View Article Online
View Journal | View Issue

Cite this: *Org. Biomol. Chem.*, 2025, **23**, 7181

Directing the chemoenzymatic assembly of desferrioxamine B as a single product using *N-tert*-butoxycarbonyl-protected substrates†

Todd E. Markham, Athavan Sresutharsan, Callum A. Rosser and Rachel Codd *

Desferrioxamine B (DFOB, **1**) is a clinical hydroxamic acid siderophore used as a chelator to treat acute and secondary iron overload disease, with further applications in metal-based radiopharmaceuticals, medicinal chemistry, and chemical biology. Its current production method uses whole-organism fermentation which results in the co-production of other hydroxamic acid analogues, and the need to purify complex mixtures to produce clinical grade **1**. Here, we have exploited the elastic properties of the *Salinispora tropica* CNB-440 recombinant NRPS-independent siderophore (NIS) synthetase DesD (*St*DesD) responsible for the late-stage biosynthesis of **1**, in combination with *N*-Boc protected substrates, to direct the production of **1** as a single product. Mixtures of *St*DesD and native amine-bearing substrates followed either a *C*-to-*N* or *N*-to-*C* directionality to assemble appreciable quantities of **1** alongside higher order homo- and/or hetero-oligomeric products. Substituting the native amine substrates for the *N*-Boc protected counterparts generated *N*-Boc protected desferrioxamine B (***N*-Boc 1**) as the sole enzyme-mediated product in exceptional yields exceeding 80%, which following an *in situ* deprotection procedure furnished **1**.

Received 16th June 2025,
Accepted 8th July 2025

DOI: 10.1039/d5ob00982k

rsc.li/obc

Introduction

Siderophores are low-molecular-weight, secondary metabolites secreted by microbial organisms that have high affinity for ferric iron (Fe^{3+}). These natural products operate to solubilise and import essential Fe^{3+} from the environment to overcome its limited bioavailability under pH neutral and aerobic conditions.[1–3] This class of natural product chelator encompasses members with different metal-binding functional groups, namely hydroxamates, catecholates, α-hydroxy-carboxylates, thiazoli(*di*)ne, *N*-nitroso-*N*-hydroxyl-amine, or mixed systems. Of this diverse collection, desferrioxamine B (DFOB, **1**) is prominent due to its listing as a World Health Organization (WHO) Essential Medicine for acute iron toxicity and secondary iron overload disease, with the latter a result of transfusion-dependent blood disorders like β-thalassemia.[4] In addition to its longstanding clinical use, **1** has an emerging profile as a metal chelator in Zr-89 radiopharmaceutical agents for immunological positron emission tomography (immuno-PET) imaging,[5–7] medicinal chemistry as an import vector for Trojan Horse antibiotic strategies,[8] and in chemical biology to probe bacterial proteomes.[4,9] Commercial production of **1** is by fermentation of Fe^{3+}-depleted *Streptomyces pilosus* cultures, which can generate other hydroxamic acid-containing siderophores as byproducts, including chain-extended **1** variants.

The co-production of other siderophore byproducts means that a series of purification steps, including removal of Fe^{3+} by competition, multiple iterations of chromatography, crystallisation, and salt metathesis,[10,11] are necessary to generate **1** in sufficient purity for clinical use. Exploring alternative approaches to access **1** could alleviate current production limitations, with the possibility of selectively generating **1** using a facile chemoenzymatic approach particularly appealing and the focus of this study.

The biosynthesis of **1** and other hydroxamic acid siderophores is regulated by the biosynthetic cluster DesABCD (Scheme 1).[12–15] This pathway begins with the decarboxylation of L-lysine by DesA, a pyridoxal 5′-phosphate (PLP)-dependent decarboxylase, generating 1,5-diaminopentane (cadaverine). DesB, an FAD-dependent amine monooxygenase, then catalyses the *N*-hydroxylation of cadaverine generating N^1-hydroxycadaverine (HC). Acyltransferase DesC next generates two different monomeric units, N^1-acetyl-N^1-hydroxycadaverine

School of Medical Sciences, Faculty of Medicine and Health, The University of Sydney, New South Wales 2006, Australia. E-mail: rachel.codd@sydney.edu.au

†Electronic supplementary information (ESI) available: Experimental details, control reaction data, MS fragmentation patterns of chemoenzymatic products, standard curves, NMR spectra of chemically synthesised compounds. See DOI: https://doi.org/10.1039/d5ob00982k

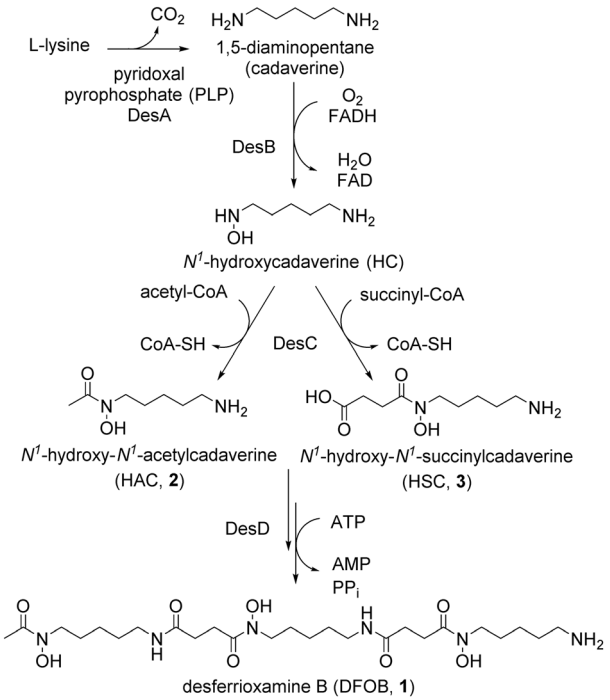

Scheme 1 DesABCD biosynthetic cascade generating **1** and other hydroxamic acid-containing siderophore byproducts (not shown).

(HAC, **2**) and N^1-succinyl-N^1-hydroxycadaverine (HSC, **3**), employing the co-factors acetyl-CoA and succinyl-CoA, respectively.[16] Finally, a nonribosomal peptide synthetase (NRPS)-independent siderophore (NIS) synthetase, DesD, catalyses iterative condensation reactions between monomers **2** and **3** to generate **1**. Onward DesD-catalysed reactions between **1** and **3** or **3** oligomers generate chain-extended **1** analogues.[17] DesD from other species, including the marine bacterium *Salinispora tropica* CNB-440 (*St*DesD), catalyse the production of sets of **3** oligomers and the cognate macrocycles.[17,18] A recent study has implicated additional enzymes in the biosynthetic pathway of **1** which are proposed to regulate the concentration of **2** and thereby **2**-dependent products, including **1**.[19]

The ability of *St*DesD to perform iterative rounds of condensation reactions suggests some degree of elasticity and relaxed substrate specificity to accommodate the growing hydroxamic acid oligomers,[17] which also accords with the broad substrate flexibility of enzyme homologues.[20,21] This enzyme plasticity has potential to be exploited in a chemoenzymatic approach by introducing non-native substrates containing bulky protecting groups to control the siderophore profile. Chemoenzymatic processes are an attractive approach to access natural products and pharmaceutical agents.[22–25] These biocatalytic processes provide benefits, particularly in relation to amide bond formation, as a green alternative to traditional chemical synthesis with increased atom economy, improved safety and lower environmental impacts.[26–28]

Here, a chemoenzymatic strategy using recombinant *St*DesD and non-native substrates containing an amine protecting group has been examined as a directed approach to produce **1** as a single product.

Results and discussion

Monomeric and dimeric hydroxamic acid substrates with free or *N*-Boc-protected amine groups were prepared synthetically using methods adapted from the literature (ESI, Scheme S1†).[29] *N*-Boc-DFOB (***N*-Boc 1**) was prepared (ESI†) as an authentic standard. Recombinant *St*DesD was generated using previously established methods (ESI, Fig. S1†)[30] and its function was confirmed by control reactions with the native substrate **3** (ESI, Fig. S2 and 3†).[17]

Typical chemoenzymatic reactions involved incubation of mixtures of *St*DesD and the co-factors $MgCl_2$ and ATP with equimolar quantities of the hydroxamic acid substrate(s) at 37 °C for 4 h. Reaction mixtures were then quenched with formic acid and analysed by LC-HRMS/MS.

Chemoenzymatic reactions using free amine-bearing substrates

Initial chemoenzymatic reactions probed the formation of **1** with *St*DesD using native substrates with free amine groups to mimic the final condensation reaction in the biosynthetic cascade. Two potential pathways exist for the generation of **1**, whereby **2** is condensed with homodimer **4** (Scheme 2a) (with **4** equivalent to **3**–**3** in which the first amide bond is formed

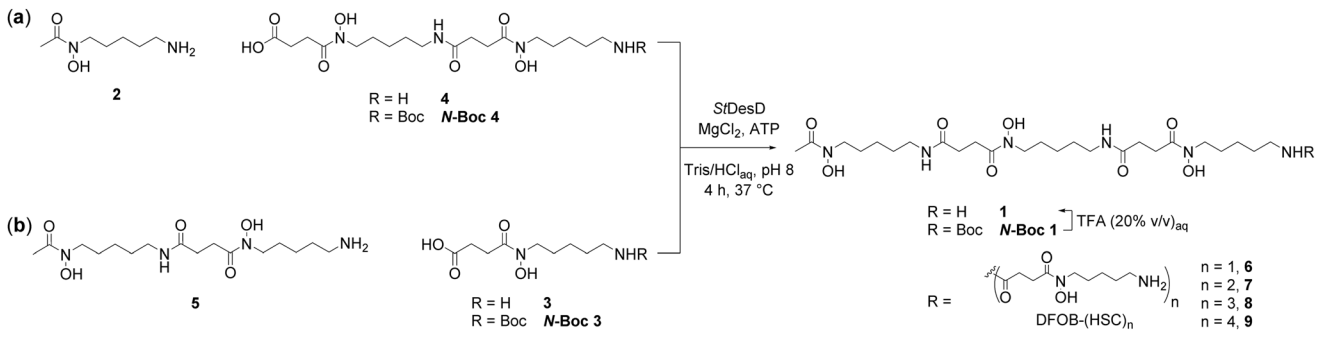

Scheme 2 Chemoenzymatic assembly of **1** employing free (**3** or **4**) or *N*-Boc protected (***N*-Boc 3** or ***N*-Boc 4**) hydroxamic acid substrates in an (a) *N*-to-*C* or (b) *C*-to-*N* direction.

proximal to the terminal amine group of the ultimate product **1** (*N*-to-*C* direction)), or **3** with heterodimer **5** (Scheme 2b) (with **5** equivalent to **2**–**3** in which the first amide bond is formed proximal to the acetyl group of the ultimate product **1** (*C*-to-*N* direction)).[31] LC-MS analysis of the reaction mixtures containing the free amine substrates **2** and **4** (Fig. 1) or **3** and **5** (Fig. 2) in the presence of *St*DesD and cofactors showed signals with *m*/*z* values attributable to enzyme-mediated product formation, as compared with the no enzyme controls, which contained signals only for residual starting materials. Since dimer **4** and monomer **3** contain flanking amine and carboxylic acid termini, each co-substrate system gave products (ESI, Fig. S2†) resulting from enzyme-mediated self-oligomerisation and ring-closing reactions. Alongside this set of homo-oligomeric and macrocyclic products, **1** and **1**-extension products were detected, as described in turn for each co-substrate system.

Reaction solutions containing *St*DesD in the presence of blunt-ended **2** and homodimer **4** as co-substrates showed the formation of **1**, oligomers of **4**, and **1**-extended oligomers, including DFOB-$(HSC)_2$ (**7**) and DFOB-$(HSC)_4$ (**9**) (Fig. 1). The formation of **1** from **2** and **4** correlates with a *N*-to-*C* biosynthetic directionality. Neither **7** nor **9** have a unique assembly pathway. The **1**-extended oligomer **7** could be assembled from the condensation of **1** (itself the condensation product of **2** and **4**) with **4**, or from **2** with $(\mathbf{4})_2$. The **1**-extended oligomer **9** could be formed from the condensation reaction between **7** and **4**, or **1** and $(\mathbf{4})_2$, or **2** and $(\mathbf{4})_3$. The identities of **7** and **9** were confirmed by MS/MS fragmentation patterns (ESI, Fig. S4†) and comparison to prior literature where similar **1**-extended oligomers were generated in reaction solutions of *St*DesD and co-substrates **1** and **3**.[17]

In comparison to the **2** and **4** co-substrate system, solutions with **3** and the heterodimer **5** showed the formation of **1** alongside three **1**-extended oligomers **6**–**8** (Fig. 2). The observation of **1** from co-substrates **3** and **5** differed from a previous study, which used the same co-substrate combination and similar reaction conditions, but did not observe **1**.[18] The formation of **1** from **3** and **5** correlates with a *C*-to-*N* biosynthetic directionality. The **1**-extended oligomers, DFOB-HSC (DFO*) **6**,[32] **7**, and DFOB-$(HSC)_3$ **8** could be formed by iterative condensation reactions of **3** with the growing **1** oligomer, or combinations of **5** with $(\mathbf{3})_2$, $(\mathbf{3})_3$, or $(\mathbf{3})_4$, or combinations of the above.

The production of **1** from each of these chemoenzymatic approaches (**2** and **4**; **3** and **5**) was quantified by using a standard curve (ESI, Fig. S5a†) and by spiking reaction solutions with an authentic standard of **1** of known concentration. Co-substrates **2** and **4** produced **1** in a 30% yield, with co-substrates **3** and **5** producing **1** in a 17% yield. Significant production of **1** was seen in both co-substrate systems, which suggests *St*DesD has capacity to assemble **1** in both the *N*-to-*C* and *C*-to-*N* directions. This gives new insight into reports that suggest the **1** assembly pathway has a directional preference,[31,33] or is uni-directional.[18]

Reactions using the homodimer **4** showed close to twice the amount of **1** produced compared to reactions using the heterodimer **5**. This could be due to the increased diffusion rate of monomer **2** than dimer **5** into the enzyme active site, thereby increasing the concentration of nucleophile for reaction with the respective AMP-activated carboxylic acid co-substrate (**4** or **3**). Alternatively, or in conjunction, differences between the

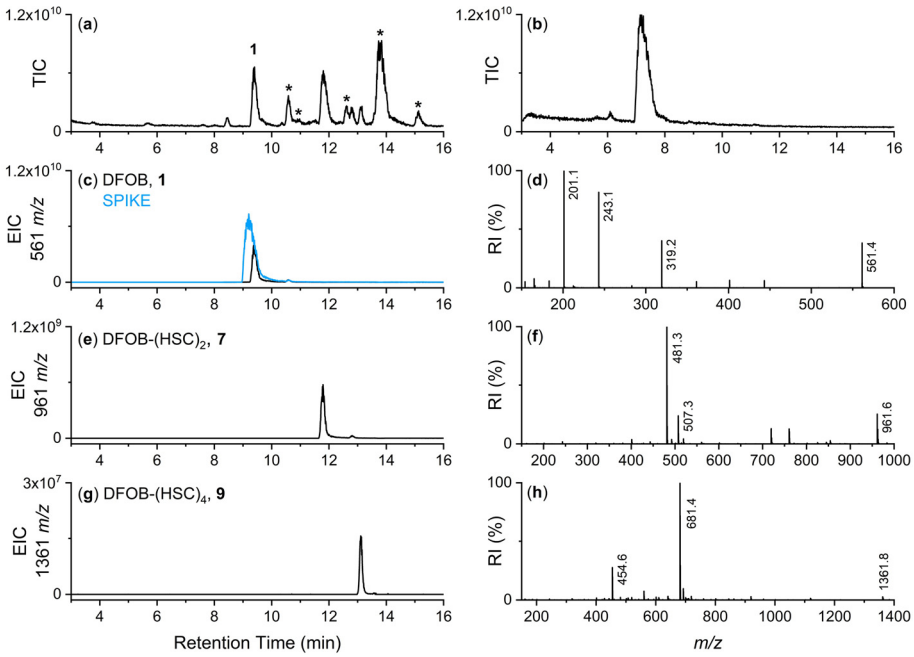

Fig. 1 LC-MS traces from solutions of **2** and **4** with $MgCl_2$ and ATP incubated (37 °C, 4 h) in the presence (a and c–h) or absence (b) of *St*DesD as detected by TIC (a and b) or shown as an EIC (c, e and g) with values set to detect the $[M + H]^+$ adducts of **1** (c), **7** (e), and **9** (g), with their corresponding mass spectra (d, f and h). Signals marked with an asterisk (*) in (a) are due to homo-oligomeric products of **4** (ESI Fig. S2†).

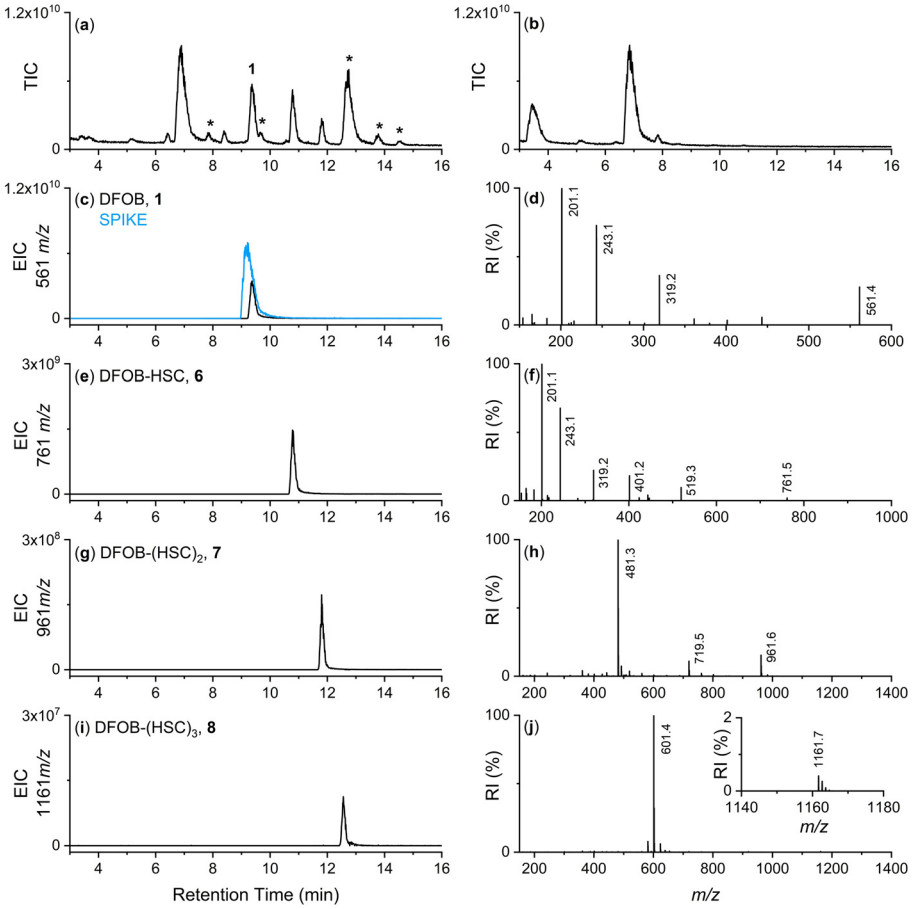

Fig. 2 LC-MS traces from solutions of **5** and **3** with $MgCl_2$ and ATP incubated (37 °C, 4 h) in the presence (a and c–j) or absence (b) of *St*DesD as detected by TIC (a and b) or shown as an EIC (c, e, g and i) with values set to detect the $[M + H]^+$ adducts of **1** (c), **6** (e), **7** (g), and **8** (i), with their corresponding mass spectra (d, f, h and j). Signals marked with an asterisk (*) in (a) are due to homo-oligomeric products of **3** (ESI, Fig. S2†).

diffusion rates, and/or reactivity of the dimer **4** and monomer **3**, including differences in self-oligomerisation and macrocyclisation, could moderate levels of the cognate AMP-activated substrate. Furthermore, we have observed the susceptibility of substrates **3** and **4** to undergo hydrolytic degradation to generate des-succinyl products that are no longer viable substrates for AMP activation. The decomposition and decreased availability of **3** and **4** would moderate the DesD-catalysed reaction profile. These potential pathways warrant further investigation using modelling and experimental approaches and informed by available DesD X-ray crystal structures.[15,34]

The complexity of the product profile using native substrates highlighted the opportunity to use *N*-protected substrates to control the chemoenzymatic assembly of **1**. Should the steric bulk of the *N-tert*-butoxycarbonyl group not impede substrate binding, the use of ***N*-Boc 3** and ***N*-Boc 4** would prevent the formation of homo-oligomers from **3** or **4** and **1**-extended oligomers to simplify the product profile and increase **1** production.

Chemoenzymatic reactions of *N*-protected substrates

Directing the chemoenzymatic assembly of **1** was interrogated by using either the *N*-Boc protected homodimer ***N*-Boc 4**, or the *N*-Boc protected monomer ***N*-Boc 3**, in reactions with the corresponding blunt-ended substrate (**2** and **5**, respectively), to drive the formation of ***N*-Boc 1** as a single product.

Solutions containing **2** and ***N*-Boc 4** with *St*DesD gave a simplified product profile (Fig. 3) compared to the chemoenzymatic reaction employing the free amine counterparts (Fig. 1). While the TIC from the LC-MS analysis of this solution (Fig. 3b) appeared to be similar with that of the no enzyme control (Fig. 3a), the EIC traces showed the formation of ***N*-Boc 1**, which was confirmed by a spike experiment using a synthesised standard (Fig. 3h). The retention time of ***N*-Boc 1** was similar to that of ***N*-Boc 4**, with efforts to resolve these co-eluting species unsuccessful. It was envisaged upon *in situ* *N*-Boc deprotection of ***N*-Boc 1** and ***N*-Boc 4** that **1** and **4** would separate.

The concentration of ***N*-Boc 1** produced in the chemoenzymatic reaction mixtures was measured using EIC traces of native solutions and following spiking with a known quantity of authentic ***N*-Boc 1**, alongside a ***N*-Boc 1** standard curve (ESI, Fig. S5b†). This analysis showed the **2** and ***N*-Boc 4** co-substrate system gave ***N*-Boc 1** in a 9% yield, which assuming a quantitative conversion to **1**, was significantly less than the 30% yield of **1** produced from the **2** and **4** co-substrate system. This indi-

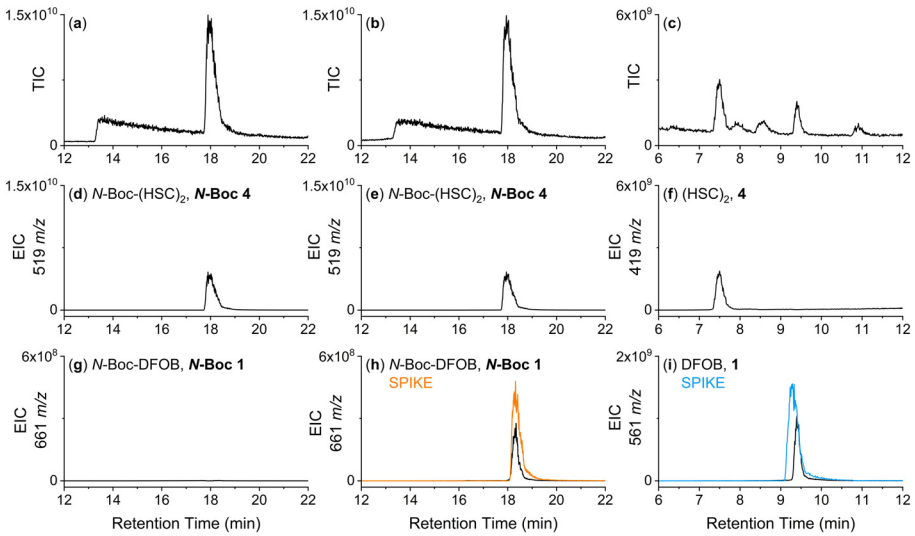

Fig. 3 LC-MS traces from solutions of **2** and ***N*-Boc 4** with $MgCl_2$ and ATP incubated (37 °C, 4 h) in the absence (a, d and g) or presence (b, e and h) of *St*DesD and then treated with TFA (c, f and i) as detected by TIC (a, b and c) or shown as an EIC (d–i) with values set to detect the $[M + H]^+$ adducts of ***N*-Boc 4** (d and e), **4** (f), ***N*-Boc 1** (g and h), and **1** (i).

cated the *N*-Boc group in ***N*-Boc 4** impeded the condensation reaction, likely due to steric interference at the enzyme active site. Furthermore, ***N*-Boc 4** was seen to degrade to a product with the loss of the C-terminal succinate group. The propensity for ***N*-Boc 4** to degrade together with its decreased aqueous solubility are probable contributors to this decreased yield. The *in situ* addition of TFA to this solution liberated **1** from ***N*-Boc 1** (Fig. 3i), which was well resolved from other reaction components. Alongside **1**, **4** was produced from the deprotection of ***N*-Boc 4** (Fig. 3f), together with the des-succinyl degradation product of **4**.

The directed chemoenzymatic assembly of **1** was next explored using co-substrates ***N*-Boc 3** and **5**. Reaction mixtures using ***N*-Boc 3** and **5** showed a simplified product profile (Fig. 4) compared to the equivalent free-amine system **3** and **5**. Furthermore, ***N*-Boc 1** (Fig. 4h) was well resolved from ***N*-Boc 3** (Fig. 4e), and was produced in higher quantities than the co-substrate system **2** and ***N*-Boc 4**.

The ***N*-Boc 3** and **5** co-substrate system generated ***N*-Boc 1** in 83% yield, which surpassed both the corresponding free amine co-substrate system with **3** and **5** (Fig. 2) and the alternative **2** and ***N*-Boc 4** co-substrate system (Fig. 3). The

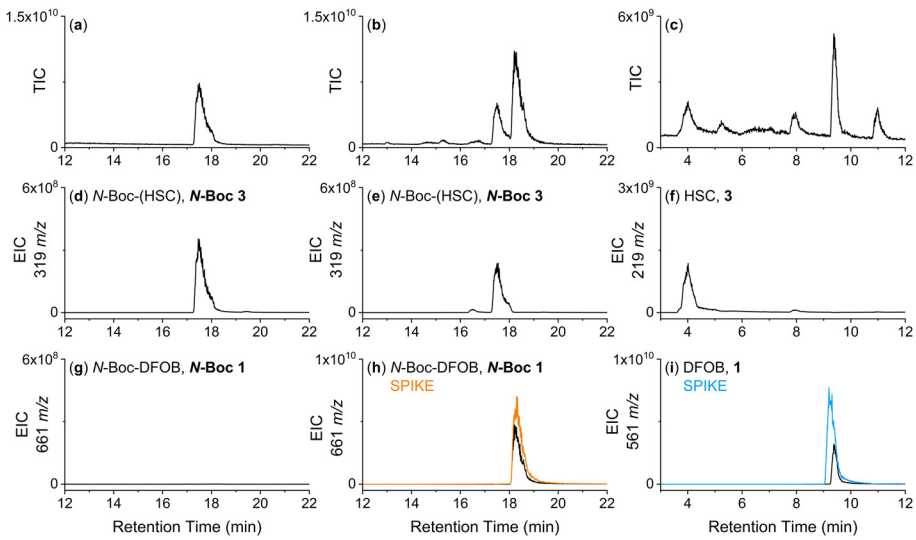

Fig. 4 LC-MS traces from solutions of **5** and ***N*-Boc 3** with $MgCl_2$ and ATP incubated (37 °C, 4 h) in the absence (a, d and g) or presence (b, e and h) of *St*DesD and then treated with TFA (c, f and i) as detected by TIC (a, b and c) or shown as an EIC (d–i) with values set to detect the $[M + H]^+$ adducts of ***N*-Boc 3** (d and e), **3** (f), ***N*-Boc 1** (g and h), and **1** (i).

Table 1 Yields of **1** or ***N*-Boc 1** from chemoenzymatic reactions using free-amine bearing substrates or *N*-protected substrates, respectively

Reaction	Direction	Yield[a] (%)
2 + **4**	*N*-to-*C*	30 (**1**)
3 + **5**	*C*-to-*N*	17 (**1**)
2 + ***N*-Boc 4**	*N*-to-*C*	9 (***N*-Boc 1**)
***N*-Boc 3** + **5**	*C*-to-*N*	83 (***N*-Boc 1**)

[a] Determined by standard curve of **1** or ***N*-Boc 1** (ESI, Fig. S5†).

increase in reaction efficiency using ***N*-Boc 3** over ***N*-Boc 4** suggests an increased affinity of ***N*-Boc 3** over ***N*-Boc 4** for the active site governing AMP activation and/or higher available concentrations of ***N*-Boc 3** than ***N*-Boc 4** due to potential differences in hydrolytic stability. The *in situ* deprotection of ***N*-Boc 1** with TFA liberated **1** (Fig. 4i) as the major product alongside small quantities of **3** and its des-succinyl degradation product. This directed approach significantly improved the yield of **1** compared to the reactions using the free amine substrates (Table 1) by preventing the ability to form **1**-extension products, and **3** and **4** homo-oligomers and macrocycles.

Conclusions

The recombinant NIS synthetase *St*DesD from *Salinispora tropica* CNB-440 was used to explore the chemoenzymatic assembly of **1** using either free amine or *N*-Boc protected substrates. Alongside, the work provided new insight into **1** assembly pathways. Chemoenzymatic reactions using substrates with free amine groups showed complex product profiles reflecting those from whole organism fermentation.[35] **1** was formed from the reaction between **2** and **4** (*N*-to-*C* direction) (yield 30%) or **3** and **5** (*C*-to-*N* direction) (yield 17%) and although yields were different, supports *St*DesD is able to assemble **1** using a bi-directional pathway, suggesting the *N*-to-*C* directionality of **1** biosynthesis proposed as universal for *Streptomyces* has a species dependence among actinomycetes.

A directed chemoenzymatic assembly approach using *N*-Boc protected amine substrates, ***N*-Boc 4** (replacing **4**) or ***N*-Boc 3** (replacing **3**) was successful in simplifying the product profile. In each instance, ***N*-Boc 1** was the single enzyme-mediated product observed and was readily deprotected *in situ* with TFA to give **1**. The trend in yield in the *N*-Boc protected system was interconverted (**2** and ***N*-Boc 4** (yield 9%); ***N*-Boc 3** and **5** (yield 83%)) compared to the matched free amine substrate systems. This remains consistent with the proposition of a bi-directional assembly pathway, although the different trends in yields and/or substrate stabilities makes it difficult to draw conclusions of a directional preference. The 83% yield of ***N*-Boc 1** from ***N*-Boc 3** and **5**, as converted to **1** upon deprotection, demonstrates the merit of using a directed chemoenzymatic approach with *N*-Boc protected substrates to generate **1** as a pure product.

Author contributions

The study was conceptualised by RC, with all authors contributing to methodology design. TEM, AS, and CAR generated the experimental data. TEM wrote the manuscript with all authors contributing to review, editing and approval of the final submission.

Conflicts of interest

There are no conflicts to declare.

Data availability

The data supporting this work are provided in the main text or are included as part of the ESI.†

Acknowledgements

The Australian Research Council (DP220100101) is acknowledged for research support. This research was facilitated by access to Sydney Mass Spectrometry and Sydney Analytical, core research facilities at the University of Sydney. The University of Sydney is gratefully acknowledged for the award of an Australian Government Research Training Program (RTP) Scholarship to AS and CAR.

References

1 M. Sandy and A. Butler, Microbial iron acquisition: Marine and terrestrial siderophores, *Chem. Rev.*, 2009, **109**, 4580–4595.
2 R. C. Hider and X. Kong, Chemistry and biology of siderophores, *Nat. Prod. Rep.*, 2010, **27**, 637–657.
3 R. Codd, in *Comprehensive Inorganic Chemistry III*, ed. V. L. Pecoraro and Z. Guo, Elsevier, Oxford, 2023, vol. 2, pp. 3–29.
4 R. Codd, T. Richardson-Sanchez, T. J. Telfer and M. P. Gotsbacher, Advances in the chemical biology of desferrioxamine B, *ACS Chem. Biol.*, 2018, **13**, 11–25.
5 J. P. Holland, V. Divilov, N. H. Bander, P. M. Smith-Jones, S. M. Larson and J. S. Lewis, ^{89}Zr-DFO-J591 for immunoPET of prostate-specific membrane antigen expression *in vivo*, *J. Nucl. Med.*, 2010, **51**, 1293–1300.
6 S. Heskamp, R. Raavé, O. C. Boerman, M. Rijpkema, V. Goncalves and F. Denat, ^{8}9Zr-Immuno-positron emission tomography in oncology: State-of-the-art ^{89}Zr radiochemistry, *Bioconjugate Chem.*, 2017, **28**, 2211–2223.
7 J. R. Dilworth and S. I. Pascu, The chemistry of PET imaging with zirconium-89, *Chem. Soc. Rev.*, 2018, **47**, 2554–2571.
8 B. Rayner, A. D. Verderosa, V. Ferro and M. A. T. Blaskovich, Siderophore conjugates to combat anti-

biotic-resistant bacteria, *RSC Med. Chem.*, 2023, **14**, 800–822.

9 J. Ni, J. L. Wood, M. Y. White, N. Lihi, T. E. Markham, J. Wang, P. T. Chivers and R. Codd, Reduction-cleavable desferrioxamine B pulldown system enriches Ni(II)-superoxide dismutase from a *Streptomyces* proteome, *RSC Chem. Biol.*, 2023, **4**, 1064–1072.

10 V. Keri, Z. Czovek and A. Mezo, Multistage process for the preparation of highly pure deferoxamine mesylate salt, *US Patent*, 6858414B2, 2005.

11 Z. Konyári, V. Kéri, A. Kovács, S. Horkay, L. Eszenyi, J. Erdélyi, I. Himesi, G. Toth, J. Bálint, J. Sziláyi, F. Vinczi, C. Szabó and N. Sas, Process for the preparation of high-purity deferoxamine salts, *Patent US*, 5374771A, 1994.

12 F. Barona-Gómez, U. Wong, A. E. Giannakopulos, P. J. Derrick and G. L. Challis, Identification of a cluster of genes that directs desferrioxamine biosynthesis in *Streptomyces coelicolor*, M145, *J. Am. Chem. Soc.*, 2004, **126**, 16282–16283.

13 N. Kadi, D. Oves-Costales, F. Barona-Gómez and G. L. Challis, A new family of ATP-dependent oligomerization-macrocyclization biocatalysts, *Nat. Chem. Biol.*, 2007, **3**, 652–656.

14 C. S. Carroll and M. M. Moore, Ironing out siderophore biosynthesis: a review of non-ribosomal peptide synthetase (NRPS)-independent siderophore synthetases, *Crit. Rev. Biochem. Mol. Biol.*, 2018, **53**, 356–381.

15 K. D. Patel, M. B. Fisk and A. M. Gulick, Discovery, functional characterization, and structural studies of the NRPS-independent siderophore synthetases, *Crit. Rev. Biochem. Mol. Biol.*, 2025, **59**, 447–471.

16 J. L. Ronan, N. Kadi, S. A. McMahon, J. H. Naismith, L. M. Alkhalaf and G. L. Challis, Desferrioxamine biosynthesis: Diverse hydroxamate assembly by substrate tolerant acyl transferase DesC, *Philos. Trans. R. Soc., B*, 2018, **373**, 20170068.

17 K. P. Nolan, C. A. Rosser, J. L. Wood, J. Font, A. Sresutharsan, J. Wang, T. E. Markham, R. M. Ryan and R. Codd, An elastic siderophore synthetase and rubbery substrates assemble multimeric linear and macrocyclic hydroxamic acid metal chelators, *Chem. Sci.*, 2025, **16**, 2180–2190.

18 J. Yang, V. S. Banas, G. S. M. Rivera and T. A. Wencewicz, Siderophore synthetase DesD catalyzes N-to-C condensation in desferrioxamine biosynthesis, *ACS Chem. Biol.*, 2023, **18**, 1266–1270.

19 H. E. Augustijn, Z. L. Reitz, L. Zhang, J. A. Boot, S. S. Elsayed, G. L. Challis, M. H. Medema and G. P. van Wezel, Genome mining based on transcriptional regulatory networks uncovers a novel locus involved in desferrioxamine biosynthesis, *PLoS Biol.*, 2025, **23**, e3003183.

20 S. Rütschlin and T. Böttcher, Dissecting the mechanism of oligomerization and macrocyclization reactions of NRPS-independent siderophore synthetases, *Chem. – Eur. J.*, 2018, **24**, 16044–16051.

21 S. Rütschlin, S. Gunesch and T. Böttcher, One enzyme to build them all: Ring-size engineered siderophores inhibit the swarming motility of *Vibrio*, *ACS Chem. Biol.*, 2018, **13**, 1153–1158.

22 S. Chakrabarty, E. O. Romero, J. B. Pyser, J. A. Yazarians and A. R. H. Narayan, Chemoenzymatic total synthesis of natural products, *Acc. Chem. Res.*, 2021, **54**, 1374–1384.

23 S. Wu, R. Snajdrova, J. C. Moore, K. Baldenius and U. T. Bornscheuer, Biocatalysis: Enzymatic synthesis for industrial applications, *Angew. Chem., Int. Ed.*, 2021, **60**, 88–119.

24 L. E. Zetzsche, S. Chakrabarty and A. R. H. Narayan, The transformative power of biocatalysis in convergent synthesis, *J. Am. Chem. Soc.*, 2022, **144**, 5214–5225.

25 T. Bayer, S. Wu, R. Snajdrova, K. Baldenius and U. T. Bornscheuer, An update: Enzymatic synthesis for industrial applications, *Angew. Chem., Int. Ed.*, 2025, e202505976, DOI: **10.1002/anie.202505976**.

26 M. Lubberink, W. Finnigan and S. L. Flitsch, Biocatalytic amide bond formation, *Green Chem.*, 2023, **25**, 2958–2970.

27 L. Bering, E. J. Craven, S. A. Sowerby Thomas, S. A. Shepherd and J. Micklefield, Merging enzymes with chemocatalysis for amide bond synthesis, *Nat. Commun.*, 2022, **13**, 380.

28 J. Pitzer and K. Steiner, Amides in nature and biocatalysis, *J. Biotechnol.*, 2016, **235**, 32–46.

29 T. E. Markham and R. Codd, A mild and modular approach to the total synthesis of desferrioxamine B, *J. Org. Chem.*, 2024, **89**, 5118–5125.

30 K. P. Nolan, J. Font, A. Sresutharsan, M. P. Gotsbacher, C. J. M. Brown, R. M. Ryan and R. Codd, Acetyl-CoA-mediated post biosynthetic modification of desferrioxamine B generates *N*- and N-*O*-acetylated isomers controlled by a pH-switch, *ACS Chem. Biol.*, 2022, **17**, 426–437.

31 T. J. Telfer, M. P. Gotsbacher, C. Z. Soe and R. Codd, Mixing up the pieces of the desferrioxamine B jigsaw defines the biosynthetic sequence catalyzed by DesD, *ACS Chem. Biol.*, 2016, **11**, 1452–1462.

32 M. Patra, A. Bauman, C. Mari, C. A. Fischer, O. Blacque, D. Haussinger, G. Gasser and T. L. Mindt, An octadentate bifunctional chelating agent for the development of stable zirconium-89 based molecular imaging probes, *Chem. Commun.*, 2014, **50**, 11523–11525.

33 T. J. Telfer and R. Codd, Fluorinated analogues of desferrioxamine B from precursor-directed biosynthesis provide new insight into the capacity of DesBCD, *ACS Chem. Biol.*, 2018, **13**, 2456–2471.

34 J. Yang, V. S. Banas, K. D. Patel, G. S. M. Rivera, L. S. Mydy, A. M. Gulick and T. A. Wencewicz, An acyl-adenylate mimic reveals the structural basis for substrate recognition by the iterative siderophore synthetase DesD, *J. Biol. Chem.*, 2022, **298**, 102166.

35 N. Ejje, C. Z. Soe, J. Gu and R. Codd, The variable hydroxamic acid siderophore metabolome of the marine actinomycete *Salinispora tropica* CNB-440, *Metallomics*, 2013, **5**, 1519–1528.